

## RESEARCH ARTICLE

# Visual detection threshold in the echolocating Daubenton's bat (*Myotis daubentonii*)

Clément Céchetto<sup>1,\*‡</sup>, Lasse Jakobsen<sup>1</sup> and Eric J. Warrant<sup>2</sup>**ABSTRACT**

All bats possess eyes that are of adaptive value. Echolocating bats have retinæ dominated by rod photoreceptors and use dim light vision for navigation, and in rare cases for hunting. However, the visual detection threshold of insectivorous echolocating bats remains unknown. Here, we determined this threshold for the vespertilionid bat *Myotis daubentonii*. We show that for a green luminous target, *M. daubentonii* has a visual luminance threshold of  $3.2(\pm 0.9) \times 10^{-4}$  cd m<sup>-2</sup>, an intensity corresponding to the luminance of an open cloudless terrestrial habitat on a starlit night. Our results show that echolocating bats have good visual sensitivity, allowing them to see during their active periods. Together with previous results showing that *M. daubentonii* has poor visual acuity ( $\sim 0.6$  cycles deg<sup>-1</sup>), this suggests that echolocating bats do not use vision to hunt but rather to orient themselves.

**KEY WORDS:** Bat vision, Absolute sensitivity, Behaviour, Nocturnal vision, Psychophysics

**INTRODUCTION**

Vision is one of the most ubiquitous senses in the animal kingdom, and almost all animal species possess eyes for detecting light, ranging from simple pit eyes in clams to the more complex compound eyes of insects and the camera eyes of mammals (Land and Fernald, 1992; Land and Nilsson, 2012). However, while vision is most efficient in bright light, it is not limited to day-active animals (Warrant, 2008).

Most bats are nocturnal and use echolocation to navigate and forage, emitting high-frequency sound pulses, and localizing and identifying objects in their surroundings by the returning echoes (Griffin, 1958). Echolocation allows bats to forage in the complete absence of light, but nonetheless all echolocating bats have eyes. While the eyes of echolocating bats are small compared with those of non-echolocating bats (Thiagavel et al., 2018), it is clear that they have functional significance because (i) eyes are exceptionally costly to maintain (Niven and Laughlin, 2008) and as a consequence are reduced (Borghi et al., 2002) or even lost over evolutionary time if unused (Jeffrey et al., 2003), and (ii) there is strong purifying selection on the opsin genes in both echolocating and non-echolocating bats (Shen et al., 2010; Zhao et al., 2009). Echolocating bats have retinæ dominated by rod photoreceptors

(Suthers and Wallis, 1970), the photoreceptor class subserving dim-light vision in all vertebrates (Ahnel and Kolb, 2000), indicating a strong adaptation to low-light conditions. However, the small size of echolocating bat eyes, both in relative terms and in absolute terms, does limit their visual sensitivity and resolution at low light intensities (Céchetto et al., 2020; Pettigrew et al., 1988; Thiagavel et al., 2018).

Visual acuity in echolocating bats appears to correlate with feeding ecology. Aerial hawking insectivorous bats have poorer visual acuity than both carnivorous and frugivorous gleaners, with values as low as 0.2 cycles deg<sup>-1</sup> in the small aerial hawk *Rhinolophus rouxi*, compared with around 2 cycles deg<sup>-1</sup> in the very large carnivorous gleaner *Megaderma gigas* (Pettigrew et al., 1988). However, the visual acuity of most aerial hawking bats is below 0.6 cycles deg<sup>-1</sup>, with one reported case at 1.3 cycles deg<sup>-1</sup> (Bell and Fenton, 1986; Céchetto et al., 2020; Eklöf et al., 2014; Suthers, 1966). Functionally this means that they can detect 30–90 mm objects at 1 m distance under ideal conditions and it is generally accepted that this is insufficient to detect and track their insect prey (Eklöf et al., 2014). This is also likely to be the underlying drive for the evolution of echolocation, as the ancestral bat probably had the auditory capacity for echolocation but not the visual capacity for high-speed aerial pursuit of insects (Thiagavel et al., 2018). It is therefore generally held that aerial hawking insectivorous bats predominantly use their eyes for large-scale orientation and navigation (Barbour et al., 1966; Boonman and Jones, 2002; Buchler and Childs, 1982; Childs and Buchler, 1981; Davis and Barbour, 1965; Eklöf et al., 2014; Kugler et al., 2019).

However, the absolute visual thresholds of echolocating bats are still largely unknown (for a summary, see Table S1). A few studies have reported the lowest luminances allowing optomotor responses (e.g.  $6 \times 10^{-4}$  cd m<sup>-2</sup> for *Macrotus californicus* and *Antrozous pallidus*: Bell and Fenton, 1986) or brightness discrimination ( $10^{-4}$  cd m<sup>-2</sup> for *Eptesicus fuscus*: Ellins and Masterson, 1974), but while such measurements may function as a good proxy, they systematically underestimate absolute sensitivity because good acuity requires higher light levels (Cronin et al., 2014; Land and Nilsson, 2012). Liu et al. (2015) used flash-evoked visual potentials to measure absolute visual threshold in *Taphozous melanopogon* (Emballonuridae) and *Rhinolophus affinis* (Rhinolophodae):  $2 \times 10^{-4}$  and  $1.2 \times 10^{-2}$  cd m<sup>-2</sup>, respectively. But such measurements need to be ground-truthed against behavioural measures as they usually result in a higher threshold than obtained in behavioural experiments. The only behavioural measure of visual sensitivity that has been made in echolocating bats is for the nectar-feeding *Glossophaga soricina* – with a peak spectral sensitivity at 510 nm (green), visual threshold was obtained at an illuminance of about  $7.6 \times 10^9$  photons cm<sup>-2</sup> s<sup>-1</sup> (Winter et al., 2003). *Glossophaga soricina* is a nectar-feeding bat that potentially uses vision (and particularly UV vision) to enhance contrast when detecting light reflected from flower petals (Guldberg and Atsatt, 1975; Horovitz

<sup>1</sup>Department of Biology, University of Southern Denmark, Campusvej 55, 5230 Odense M, Denmark. <sup>2</sup>Department of Biology, Lund University, Biology Building, Sölvegatan 35, 223 62 Lund, Sweden.

\*Present address: The Graduate University for Advanced Studies, SOKENDAI, Shonan Village, Hayama, Kanagawa 240-0193, Japan.

‡Author for correspondence (clement.cechetto@pm.me)

 C.C., 0000-0001-8681-6366

and Cohen, 1972). Moreover, this family of bats (*Phyllostomidae*) have larger eyes relative to their body size than other insectivorous echolocating bats (Thiagavel et al., 2018).

Hence, the aim of our study was to behaviourally determine the visual detection threshold in an insectivorous echolocating bat. We hypothesized that non-gleaning insectivorous bats have poor acuity, but a relatively good visual sensitivity that allows large-scale orientation and navigation under open-sky conditions. To test this hypothesis, we used operand conditioning to determine the visual detection threshold of a vespertilionid bat for which we already have data on visual acuity: *Myotis daubentonii* (Céchetto et al., 2020). *Myotis daubentonii* is a small insectivorous bat (8–10 g) that hunts at low altitude over water. It starts hunting from around 30 min after sunset and continues for about 1–2 h (Rydell et al., 1996; Encarnação and Dietz, 2006).

## MATERIALS AND METHODS

### Animals

We captured four adult male *Myotis daubentonii* (Kuhl 1817) in the vicinity of Odense in Denmark, with permission from the Danish Environmental Protection Agency (permit number: NST-3446-00001). The animals were kept on a reversed 8 h:16 h day:night cycle with a stable temperature of 20°C and 60% humidity and were released following experiments.

### Apparatus

Experiments were conducted in a Y-maze, with a floor made of black felt, and walls made of aluminium painted with matt black paint. Both arms of the maze were covered with a black-painted aluminium roof and further covered with felt to prevent any exterior light from entering. The maze itself was in a small room that was completely dark during experiments.

Each arm measured 15 cm in length from the bifurcation point and was 12 cm wide and 12 cm high. The common arm also measured 15 cm in length and was 15 cm wide and 12 cm high (Fig. 1A). We used a small red headlight only when necessary and the computer screen was dimmed with a neutral density (ND) filter sheet of ND value 2.

The Y-maze was equipped with a broad green (peak 565 nm) LED light source (Broadcom HLMP-3950: RS Components #590-525) (spectrum shown in Fig. 1B); the spectrum was measured from the inside of the labyrinth arm after passing through the diffusing paper) and two custom-made filter wheels, containing seven 12.5 mm diameter UV-VIS quartz ND filters from Edmund Optics (with ND values of 0.3, 0.6, 0.9, 1.3, 2, 2.5, 3). The filter wheels were activated by servo motors (Parallax Standard Servo #900-00005) controlled by an Arduino Uno board. A 2-pole bifurcated liquid light guide (Uvitron UV2168) carried light to two diffusing filters (Lee filters 216 white diffusion) that, when illuminated, constituted the visual targets in each arm, each of which was round and had a diameter of 10 cm (Fig. 1B). Electronic shutters allowed the illuminated targets in each arm of the Y-maze to be turned on and off. Laser diodes (650 nm), with corresponding sensors (DFRobot LX1972), created a thin light beam across the interior of the Y-maze arm that, when broken, detected when a bat entered the arm to make its choice, thereby triggering the acquisition of that decision.

The different light intensities used (given as spectral radiance in  $\text{mW m}^{-2} \text{sr}^{-1} \text{nm}^{-1}$ ), created by a combination of one or two ND filters, are reported in Table 1. The first five light levels were measured using a Ramses hyperspectral radiometer (TriOS Optical Sensors). We used the given ND values of the filters to calculate the

intensity of the dimmer light levels (beyond the range of the radiometer) as the radiometric measurements at brighter light levels did not differ from the calculated values. To convert spectral radiance into  $\text{cd m}^{-2}$  we used the following formula (BIPM, 2006; Johnsen, 2012):

$$\text{cd m}^{-2} = 683 \sum_{\lambda=500}^{\lambda=650} E(\lambda) \hat{v}(\lambda) \Delta\lambda, \quad (1)$$

where  $E(\lambda)$  represents the photon energy spectrum,  $\hat{v}(\lambda)$  represents the scotopic human spectral sensitivity curve and  $\Delta\lambda$  is the width (in nm) of the summation step used (in our case  $\Delta\lambda=10$  nm). The wavelength limits of the summation (500–650 nm) were chosen to capture the radiance spectrum of our experimental target (Fig. 1B).

### Experimental protocol

We used a two-way forced choice paradigm (Kingdom, 2012) with a weighted staircase method (1 step down, 2 steps up) to determine the bats' detection threshold for green (~560 nm) light.

The bats were trained to go towards the arm of the Y-maze where light was present. We used positive reinforcement with a bridging signal (i.e. a buzz sound classically conditioned to be associated with food) and rewards consisting of half mealworms (larvae of *Tenebrio molitor*). After each successful trial (Hit), the light level was decreased by one step, and in the case of an unsuccessful trial (Miss), the light level was increased by 2 steps (see Table 1). We used a weighted staircase method so that if a bat was lucky in guessing the arm with the light and thus moved towards light intensities under its threshold it would be faster for it to return to visible stimulus intensities, ensuring higher motivation and reward frequency (Garcia-Perez, 1998).

Each session ended after a pre-set number of trials depending on the bat's body mass before the experiment (usually around 30 trials); if the bat's body mass was high (above ~9 g), the number of trials was reduced to ensure that the bat would finish the session. Each session started with a warm-up period, where the bat had to make four correct choices in a row for the intensity to start decreasing. This was to ensure the bat was under stimulus control, and that the bats were motivated enough by the reward to make choices and participate in the experiment. Each session also ended with a cool-down period with light intensity at the highest level (step 0 in Table 1) for the last four trials.

All recording sessions were double-blind such that neither the experimenter nor the animal could predict which arm would be illuminated for any given trial. We controlled the setup using an Arduino board controlled through serial communication using a custom-written program in Python 2.7.

At the beginning of each session, the bat was placed at the entrance to the Y-maze (Fig. 1A) and the experimenter started the first trial. The program then generated a pseudo-random sequence of stimulation in the left and right Y-maze arms so that the illumination would never be presented more than 3 times in a row in a given arm and that each arm was illuminated equally often (i.e. ~50% of the time). The program then sent instructions to the Arduino board as to which arm should be lit and at what intensity. The Arduino board selected the correct set of filters (Fig. 1A), opened the shutter on the arm to be lit, and turned on the light source and two laser triggers on each arm of the maze. To avoid giving confounding auditory cues to the bats, each side had a real and a mock shutter that would always be activated on each trial so that there was sound on both sides for every trial.

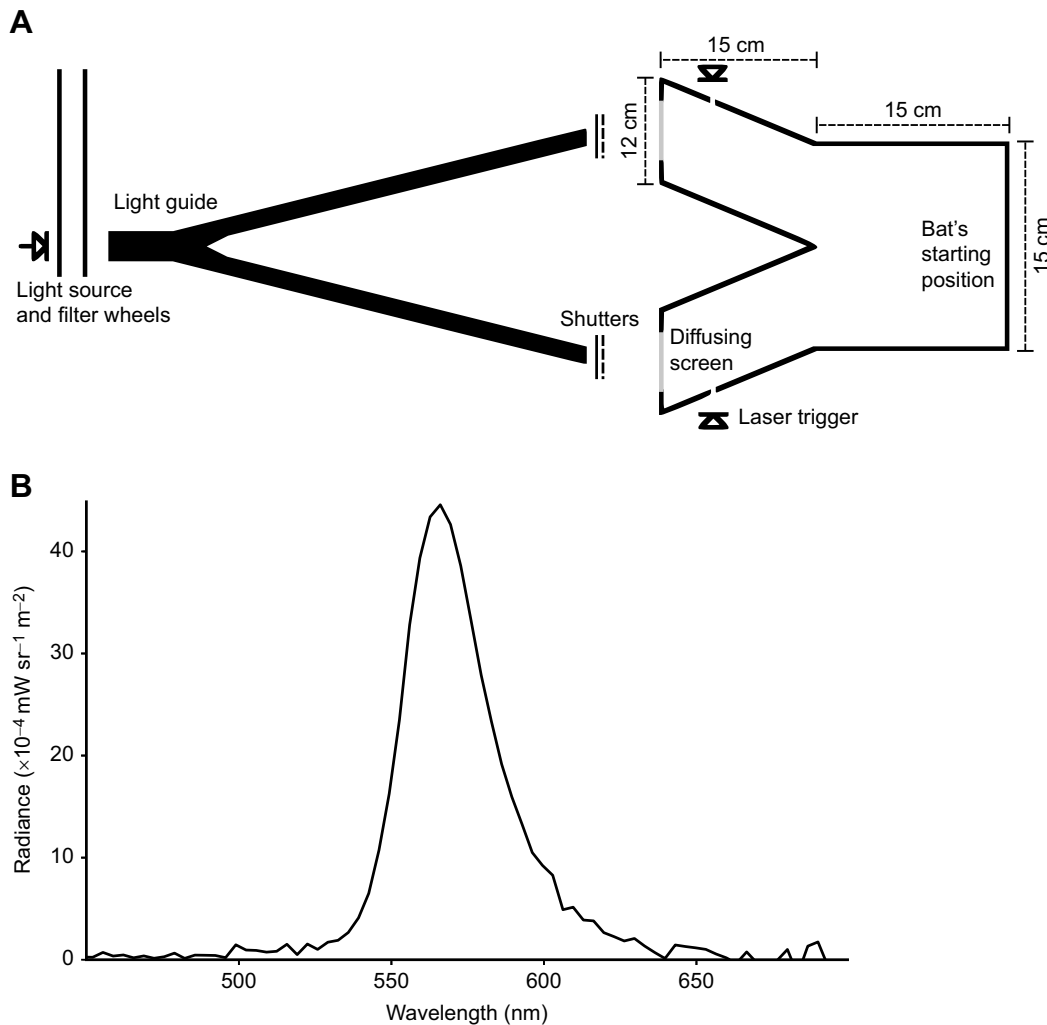


**Fig. 1. Experimental setup.** (A) Top view of the apparatus. At the end of each maze arm is a diffusing screen (light grey line), where the visual target would appear. Each pair of shutters consists of a real shutter (solid line) and a mock shutter (dashed line). The bifurcated liquid light guide (Uvitron UV21268) splits the light from the light source (LED) into two equal beams. The two filter wheels hold seven UV-VIS 12.5 mm diameter quartz neutral density (ND) filters. Laser triggers for detecting bat choices were produced using a laser diode (5 mW, 650 nm) that created a laser beam detected by an analog light sensor. The bat was detected when it broke the laser beam during approaches towards the light stimulus in a given arm. (B) The spectral radiance of the LED light source used for the stimulus measured from inside the maze arm after the diffusing paper with no ND filter in front of the light source.

The Arduino board then waited for the bat to make a choice (to cross one of the laser triggers). As soon as that happened, the light source was turned off and both shutters closed. If the bat chose correctly during the trial (Hit), the bridging signal played – the experimenter then gave the bat a reward and moved it back to the start of the maze. If the result of the trial was a Miss, the bat was simply moved back to the start of the maze. This was done using touch or, in some cases, indirect lighting from a dim red headlight. The Arduino board then sent the result of the trial (Hit or Miss) to the program and a new trial was started.

For the next trial, based on the outcome of the previous trial(s), the program determined at which intensity, and in which arm, the stimulus would next appear, and the process was repeated.

### Statistical analysis

The results of each session were saved as a comma-separated file and then analysed using a custom-written Python script using Matplotlib (<https://matplotlib.org/>) and Scipy (<https://scipy.org>) packages. Because we used a staircase method, the number of trials where a given intensity was presented during a session could be

quite low, especially at lower light intensities. Therefore, to estimate the probability of success at a given intensity as accurately as possible, we pooled results together from all sessions and calculated the probability of success for each intensity.

As the experiment used a two-way forced choice paradigm, if we had no data for a given intensity (i.e. the bat never reacted to that intensity) we set the probability to chance level (i.e. 0.5). We then used the Weibull cumulative distribution function, and least squares fitting, to generate a sigmoidal psychometric function (Kershaw, 1985; Wetherill and Levitt, 1965) that fitted the relationship between the probability of choice success  $P$  and the base-10 logarithm of target luminance  $I$ :

$$P = g + (1 - g) \times \left( 1 - e^{-\left(\frac{I}{\alpha}\right)^\beta} \right), \quad (2)$$

where  $g$  is the expected probability of success at chance level (i.e. 0.5), and  $\alpha$  and  $\beta$  control the slope of the function. The threshold

**Table 1. Light level steps used in the staircase procedure**

Step	Filter	Light level	
		$\text{mW m}^{-2} \text{nm}^{-1} \text{sr}^{-1}$	$\text{cd m}^{-2}$
0	None	$3.22 \times 10^{-3*}$	$2.16 \times 10^{-2}$
1	$10^{-0.3}$	$2.04 \times 10^{-3*}$	$1.08 \times 10^{-2}$
2	$10^{-0.6}$	$8.44 \times 10^{-4*}$	$5.43 \times 10^{-3}$
3	$10^{-0.9}$	$5.50 \times 10^{-4*}$	$2.72 \times 10^{-3}$
4	$10^{-1.3}$	$2.09 \times 10^{-4*}$	$1.08 \times 10^{-3}$
5	$10^{-1.6}$	$8.09 \times 10^{-5}$	$5.43 \times 10^{-4}$
6	$10^{-1.9}$	$4.05 \times 10^{-5}$	$2.72 \times 10^{-4}$
7	$10^{-2}$	$3.22 \times 10^{-5}$	$2.16 \times 10^{-4}$
8	$10^{-2.1}$	$2.56 \times 10^{-5}$	$1.72 \times 10^{-4}$
9	$10^{-2.5}$	$1.02 \times 10^{-5}$	$6.83 \times 10^{-5}$
10	$10^{-2.8}$	$5.10 \times 10^{-6}$	$3.42 \times 10^{-5}$
11	$10^{-3}$	$3.22 \times 10^{-6}$	$2.16 \times 10^{-5}$
12	$10^{-3.1}$	$2.56 \times 10^{-6}$	$1.72 \times 10^{-5}$
13	$10^{-3.3}$	$1.61 \times 10^{-6}$	$1.08 \times 10^{-5}$
14	$10^{-3.4}$	$1.28 \times 10^{-6}$	$8.60 \times 10^{-6}$
15	$10^{-3.6}$	$8.09 \times 10^{-7}$	$5.43 \times 10^{-6}$
16	$10^{-3.9}$	$4.05 \times 10^{-7}$	$2.72 \times 10^{-6}$
17	$10^{-4.5}$	$1.02 \times 10^{-7}$	$6.83 \times 10^{-7}$
18	$10^{-5}$	$3.22 \times 10^{-8}$	$2.16 \times 10^{-7}$

Filter represents the neutral density filter placed in front of the light source to attenuate it, and the resulting light level is presented in both  $\text{mW m}^{-2} \text{sr}^{-1} \text{nm}^{-1}$  and  $\text{cd m}^{-2}$  (calculated using Eqn 1). Light level values marked by an asterisk are the directly measured values – those not marked by an asterisk are calculated using the filter attenuation values.

was obtained by calculating the value of target luminance corresponding to a probability of success of 75% using the psychometric function previously calculated.

We also estimated the threshold by calculating the average intensity levels generating reversals (i.e. the trials where the bats missed).

## RESULTS

We calculated visual thresholds using between 6 and 12 sessions and between 142 and 385 trials with an average of 239 trials for each of the four bats (Table S2). Measurements of psychometric functions for each of the bats revealed a median threshold ( $\pm$ median absolute deviation) of  $3.2(\pm 0.9) \times 10^{-4} \text{ cd m}^{-2}$  (Fig. 2; Tables S2, S3). Likewise, when calculating the threshold using the average of reversals, we found a median threshold of  $2.0(\pm 0.3) \times 10^{-4} \text{ cd m}^{-2}$ .

## DISCUSSION

We find a luminance threshold for *M. daubentonii* of  $3.2(\pm 0.9) \times 10^{-4} \text{ cd m}^{-2}$  [ $2.0(\pm 0.3) \times 10^{-4} \text{ cd m}^{-2}$  based on average of reversals] for green light in the three most sensitive individuals, which is equivalent to the luminance of terrestrial objects in an open habitat under a moonless clear starlit sky (Warrant, 2008). This means that *M. daubentonii* should be fully capable of large-scale visual navigation and orientation under most natural conditions. However, with an estimated maximal acuity of  $0.6 \text{ cycles deg}^{-1}$ ,

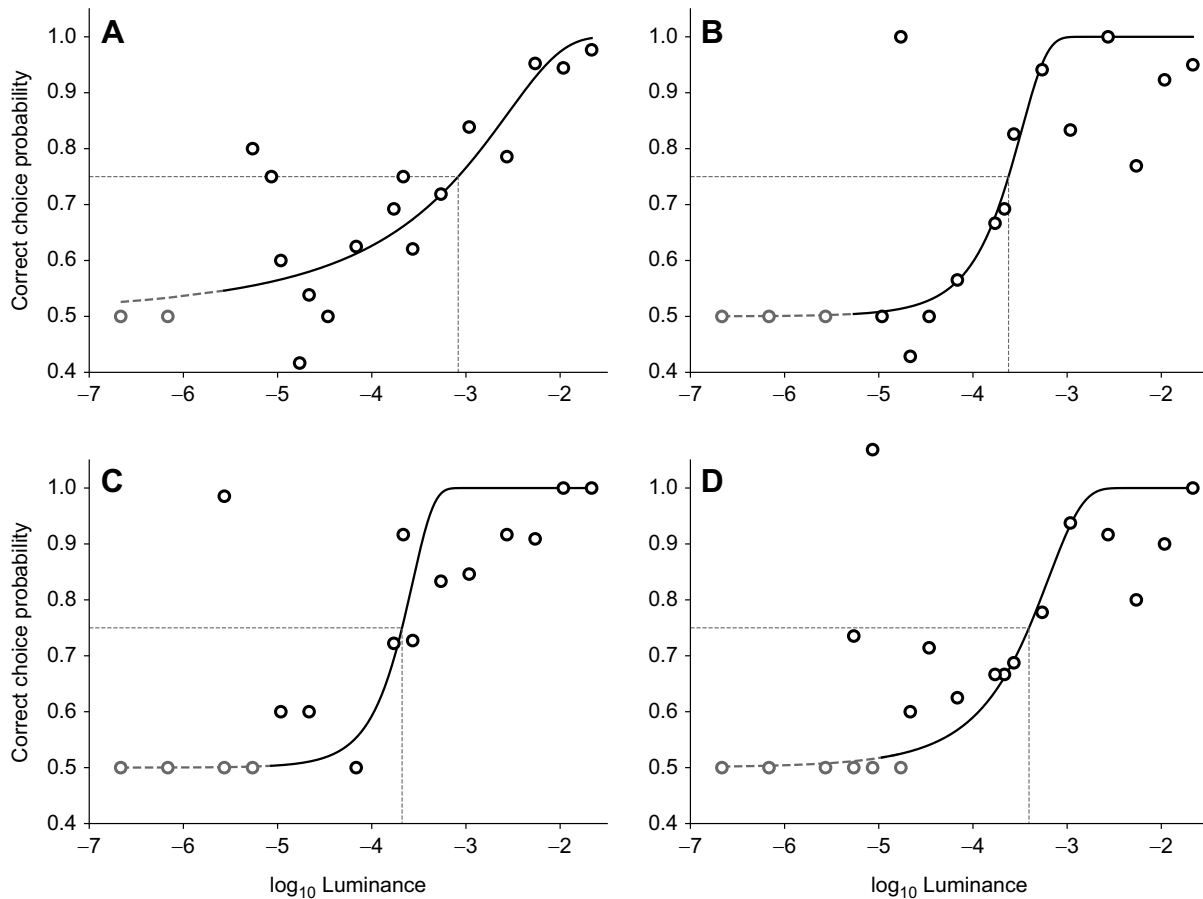


**Fig. 2. Psychometric functions for the Daubenton's bats (*Myotis daubentonii*) used in this study.** The probability of a correct choice is given as a function of the base-10 logarithm of luminance ( $\text{cd m}^{-2}$ ) for the four bats (A–D). Each data point (circles) represents the observed probability of a correct choice at that light level. The black curve is the best-fit Weibull density function (Eqn 2) describing the psychometric function. The dashed grey part of the line and grey circles represent where the probability was set to chance level (i.e. 0.5). Horizontal and vertical dashed lines indicate estimates of the intensity threshold (parameter  $\alpha$  in the Weibull function).

they are probably not capable of visually guided prey capture (Céchetto et al., 2020). Our results are consistent with existing knowledge on *Macrotus californicus*, *A. pallidus* and *E. fuscus* (Bell and Fenton, 1986; Ellins and Masterson, 1974). While these studies did not measure detection thresholds, the light levels measured that allow spatial vision and brightness discrimination are of the same order of magnitude as our measurements ( $6 \times 10^{-4}$  cd m $^{-2}$  for *M. californicus* and *A. pallidus* and  $10^{-4}$  cd m $^{-2}$  for *E. fuscus*). Compared with sensitivity measurements using visually evoked potentials, our results are on par with those obtained in *Taphozous melanopogon* ( $2 \times 10^{-4}$  cd m $^{-2}$ ) but are substantially lower than values obtained in *Rhinolophus affinis* (around  $1.2 \times 10^{-2}$  cd m $^{-2}$ ; Liu et al., 2015). Given that emballonurids have much larger eyes than rhinolophids and vespertilionids (Thiagavel et al., 2018), visually evoked potentials may underestimate the visual threshold substantially, as we think it likely that *R. affinis* has a similar threshold to *M. daubentonii* while *T. melanopogon* could be more sensitive. In their study, Winter et al. (2003) find that *G. soricina* has a relatively low threshold for detecting both green and UV light. Although their results are not directly comparable to ours, they suggest that *G. soricina* has a sufficiently low visual threshold to permit foraging from flowers at night.

The broad green light source used in our study has a wavelength peak at 560 nm, which is higher than the peak sensitivity of rhodopsin (~500 nm). Even though the emission spectrum widely overlapped the absorption spectrum of rhodopsin, had we had the possibility to use a light source that peaked at 500 nm it is likely that the detection threshold of *M. daubentonii* would have been slightly lower. Similarly, the use of a more natural stimulus may have yielded a lower threshold. Indeed, in mice it has been shown that visual performance is dependent on the ecological relevance of the stimulus (Hoy et al., 2016).

Nonetheless, this threshold indicates that the eyes of these bats are quite sensitive to light, although compared with flying foxes (family Pteropodidae) and other nocturnal mammals such as cats, the threshold is at least 3 orders of magnitude higher (i.e. less sensitive) to light (Gunter, 1951; Liu et al., 2015). In mice, whose eyes are slightly bigger than those of *M. daubentonii* (~3.5 mm versus ~1.5 mm), visual threshold is only about an order of magnitude lower (i.e. more sensitive) than that measured in *M. daubentonii* (De Tejada et al., 1997). While additional specializations, such as a tapetum lucidum (found in cats and many flying foxes), may account for part of this difference, it is likely that the substantially larger eyes and lower ocular F-number found in cats accounts for most of the difference. For example, the F-number of the cat's dark-adapted eye is 0.9 (Cronin et al., 2014) while in *Myotis sodalis* it is around 2.2 (calculated from Suthers and Wallis, 1970). This difference in F-number implies that the image formed on the retina of the cat is  $(2.2/0.9)^2 \approx 6$  times brighter than the image formed on the retina of the bat.

In echolocating bats, visual acuity appears to be correlated with feeding ecology. For instance, acuity is higher in gleaners, which have comparably larger eyes, than in aerial hawking bats (Eklöf et al., 2014; Thiagavel et al., 2018; Veilleux and Kirk, 2014). Given the sparsity of visual detection threshold data for echolocating bats, it remains to be seen if visual sensitivity likewise correlates with feeding ecology. The inherent trade-off between acuity and sensitivity would indicate that, at least in small bats such as *P. auritus* and *M. daubentonii*, it is unlikely that both sensitivity and acuity can be maximized given their relatively and absolutely small eye size (Eklöf et al., 2014). However, in larger gleaners (or in

families with larger eyes, e.g. phyllostomids or emballonurids: Thiagavel et al., 2018) sensitivity and acuity could both be high.

Our results have obvious implications for understanding vision in echolocating bats and afford us insight into how echolocating bats might use vision for navigation. But our results also have implications for conservation and habitat protection – with the urbanization of rural landscapes (Antrop, 2004), light pollution becomes another challenge that nocturnal animals must face. Indeed, light pollution has been shown to have an adverse effect on numerous bat species, ranging from general avoidance behaviour to changes in emergence behaviour, disruption of the circadian rhythm, disruption of hibernation and roost abandonment (Stone and Harris, 2015). In-depth knowledge of visual sensitivity in bat species adversely affected by light pollution should provide much needed data on how to efficiently mitigate such effects.

#### Acknowledgements

We dedicate this article to the late Professor Annemarie Surlykke, who made valuable contributions to this project.

#### Competing interests

The authors declare no competing or financial interests.

#### Author contributions

Conceptualization: C.C., L.J., E.J.W.; Methodology: C.C., L.J.; Software: C.C.; Validation: C.C., L.J., E.J.W.; Formal analysis: C.C.; Investigation: C.C.; Resources: L.J.; Writing - original draft: C.C., L.J.; Writing - review & editing: C.C., L.J., E.J.W.; Visualization: C.C., L.J., E.J.W.; Supervision: L.J., E.J.W.; Project administration: L.J.; Funding acquisition: L.J.

#### Funding

This work was funded in part by the Human Frontier Science Program and by Danmarks Frie Forskningsfond.

#### Data availability

All relevant data can be found within the article and its supplementary information.

#### References

- Ahnelt, P. K. and Kolb, H. (2000). The mammalian photoreceptor mosaic-adaptive design. *Prog. Retin. Eye Res.* **19**, 711-777. doi:10.1016/S1350-9462(00)00012-4
- Antrop, M. (2004). Landscape change and the urbanization process in Europe. *Landsc. Urban Plann.* **67**, 9-26. doi:10.1016/S0169-2046(03)00026-4
- Barbour, R. W., Davis, W. H. and Hassell, M. D. (1966). The need of vision in homing by *Myotis sodalis*. *J. Mammal.* **47**, 355-357. doi:10.2307/1378156
- Bell, G. P. G. and Fenton, M. B. (1986). Visual acuity, sensitivity and binocularity in a gleaner insectivorous bat, *Macrotus californicus* (Chiroptera: Phyllostomidae). *Anim. Behav.* **34**, 409-414. doi:10.1016/S0003-3472(86)80110-5
- BIPM. (2006). 2. Unités SI. In *Le système international d'unités* (ed. BIPM), pp. 115-116. Sèvres: STEDI Media, Paris.
- Boonman, A. and Jones, G. (2002). Intensity control during target approach in echolocating bats; stereotypical sensori-motor behaviour in Daubenton's bats, *Myotis daubentonii*. *J. Exp. Biol.* **205**, 2865-2874. doi:10.1242/jeb.205.18.2865
- Borghini, C. E., Giannoni, S. M. and Roig, V. G. (2002). Eye reduction in subterranean mammals and eye protective behavior in *Ctenomys*. *Mastozoología Neotropical* **9**, 123-134.
- Buchler, E. R. and Childs, S. B. (1982). Use of the post-sunset glow as an orientation cue by big brown bats (*Eptesicus fuscus*). *J. Mammal.* **63**, 243-247. doi:10.2307/1380633
- Céchetto, C., de Busserolles, F., Jakobsen, L. and Warrant, E. J. (2020). Retinal ganglion cell topography and spatial resolving power in echolocating and non-echolocating bats. *Brain Behav. Ecol.* **95**, 58-68. doi:10.1159/000508863
- Childs, S. B. and Buchler, E. R. (1981). Perception of simulated stars by *Eptesicus fuscus* (Vespertilionidae): A potential navigational mechanism. *Anim. Behav.* **29**, 1028-1035. doi:10.1016/S0003-3472(81)80056-5
- Cronin, T. W., Johnsen, S., Marshall, N. J. and Warrant, E. J. (2014). *Visual Ecology*. Princeton University Press.
- Davis, W. H. and Barbour, R. W. (1965). The use of vision in flight by the bat *Myotis sodalis*. *Am. Midl. Nat.* **74**, 497-499. doi:10.2307/2423278
- De Tejada, P. H., Tedó, C. M. and Costi, C. (1997). Behavioral estimates of absolute visual threshold in mice. *Vision Res.* **37**, 2427-2432. doi:10.1016/S0042-6989(97)00048-5

- Eklöf, J., Šuba, J., Petersons, G. and Rydell, J. (2014). Visual acuity and eye size in five European bat species in relation to foraging and migration strategies. *Environ. Exp. Biol.* **12**, 1-6.
- Ellins, S. R. and Masterson, F. A. (1974). Brightness discrimination thresholds in the bat, *Eptesicus fuscus*. *Brain Behav. Evol.* **9**, 248-263. doi:10.1159/000123669
- Encarnação, J. A. and Dietz, M. (2006). Estimation of food intake and ingested energy in Daubenton's bats (*Myotis daubentonii*) during pregnancy and spermatogenesis. *Eur. J. Wildlife Res.* **52**, 221-227. doi:10.1007/s10344-006-0046-2
- García-Pérez, M. A. (1998). Forced-choice staircases with fixed step sizes: asymptotic and small-sample properties. *Vision Res.* **38**, 1861-1881. doi:10.1016/S0042-6989(97)00340-4
- Griffin, D. R. (1958). *Listening in the Dark*. Yale University Press.
- Guldborg, L. D. and Atsatt, P. R. (1975). Frequency of reflection and absorption of ultraviolet light in flowering plants. *Am. Midl. Nat.* **93**, 35-43. doi:10.2307/2424103
- Gunter, R. (1951). The absolute threshold for vision in the cat. *J. Physiol.* **114**, 8-15. doi:10.1113/jphysiol.1951.sp004599
- Horowitz, A. and Cohen, Y. (1972). Ultraviolet reflectance characteristics in flowers of crucifers. *Am. J. Bot.* **59**, 706-713. doi:10.1002/j.1537-2197.1972.tb10143.x
- Hoy, J. L., Yavorska, I., Wehr, M. and Niell, C. M. (2016). Vision drives accurate approach behavior during prey capture in laboratory mice. *Curr. Biol.* **26**, 3046-3052. doi:10.1016/j.cub.2016.09.009
- Jeffrey, W. R., Strickler, A. G. and Yamamoto, Y. (2003). To see or not to see: evolution of eye degeneration in Mexican blind cavefish. *Integr. Comp. Biol.* **43**, 531-541. doi:10.1093/icb/43.4.531
- Johnsen, S. (2012). *The Optics of Life: A Biologist's Guide to Light in Nature*. Princeton University Press.
- Kershaw, C. D. (1985). Statistical properties of staircase estimates from two interval forced choice experiments. *Br. J. Mathematical Stat. Psychol.* **38**, 35-43. doi:10.1111/j.2044-8317.1985.tb00814.x
- Kingdom, F. A. A. (2012). Psychophysics. In *Encyclopedia of Human Behavior*, 2nd edn (ed. V. S. Ramachandran), pp. 234-239. San Diego: Academic Press.
- Kugler, K., Luksch, H., Peremans, H., Vanderelst, D., Wiegrebe, L. and Firzlauff, U. (2019). Optic and echo-acoustic flow interact in bats. *J. Exp. Biol.* **222**, jeb195404. doi:10.1242/jeb.195404
- Land, M. F. and Fernald, R. D. (1992). The Evolution of Eyes. *Annu. Rev. Neurosci.* **15**, 1-29. doi:10.1146/annurev.ne.15.030192.000245
- Land, M. F. and Nilsson, D.-E. (2012). *Animal Eyes*, 2nd edn, pp. 1-22, 46-71. Oxford: Oxford University Press.
- Liu, H.-Q., Wei, J.-K., Li, B., Wang, M.-S., Wu, R.-Q., Rizak, J. D., Zhong, L., Wang, L., Xu, F.-Q., Shen, Y.-Y. et al. (2015). Divergence of dim-light vision among bats (order: Chiroptera) as estimated by molecular and electrophysiological methods. *Sci. Rep.* **5**, 11531. doi:10.1038/srep11531
- Niven, J. E. and Laughlin, S. B. (2008). Energy limitation as a selective pressure on the evolution of sensory systems. *J. Exp. Biol.* **211**, 1792-1804. doi:10.1242/jeb.017574
- Pettigrew, J. D., Dreher, B., Hopkins, C. S., McCall, M. J. and Brown, M. (1988). Peak density and distribution of ganglion cells in the retinae of microchiropteran bats: implications for visual acuity. *Brain Behav. Evol. Behav.* **32**, 39-56. doi:10.1159/000116531
- Rydell, J., Entwistle, A. and Racey, P. A. (1996). Timing of foraging flights of three species of bats in relation to insect activity predation risk activity. *Oikos* **76**, 243-252. doi:10.2307/3546196
- Shen, Y.-Y., Liu, J., Irwin, D. M. and Zhang, Y.-P. (2010). Parallel and convergent evolution of the dim-light vision gene RH1 in bats (Order: Chiroptera). *PLoS ONE* **5**, e8838. doi:10.1371/journal.pone.0008838
- Stone, E. L., Harris, S. and Jones, G. (2015). Impacts of artificial lighting on bats: a review of challenges and solutions. *Mammal. Biol.* **80**, 213-219. doi:10.1016/j.mambio.2015.02.004
- Suthers, R. A. (1966). Optomotor responses by echolocating bats. *Science (New York, N.Y.)* **152**, 1102-1104. doi:10.1126/science.152.3725.1102
- Suthers, R. A. and Wallis, N. E. (1970). Optics of the eyes of echolocating bats. *Vision Res.* **10**, 1165-1173. doi:10.1016/0042-6989(70)90034-9
- Thiagavel, J., Cécchetto, C., Santana, S. E., Jakobsen, L., Warrant, E. J. and Ratcliffe, J. M. (2018). Auditory opportunity and visual constraint enabled the evolution of echolocation in bats. *Nat. Commun.* **9**, 98. doi:10.1038/s41467-017-02532-x
- Veilleux, C. C. and Kirk, E. C. (2014). Visual acuity in mammals: effects of eye size and ecology. *Brain Behav. Evol.* **83**, 43-53. doi:10.1159/000357830
- Warrant, E. J. (2008). Nocturnal vision. In *The Senses: A Comprehensive Reference*, Vol. 2 (ed. T. Albright and R. H. Masland), pp. 53-86. Elsevier.
- Wetherill, G. B. and Levitt, H. (1965). Sequential estimation of points on a psychometric function. *Br. J. Mathematical Stat. Psychol.* **18**, 1-10. doi:10.1111/j.2044-8317.1965.tb00689.x
- Winter, Y., López, J. and Von Helversen, O. (2003). Ultraviolet vision in a bat. *Nature* **425**, 612-614. doi:10.1038/nature01971
- Zhao, H., Xu, D., Zhou, Y., Flanders, J. and Zhang, S. (2009). Evolution of opsin genes reveals a functional role of vision in the echolocating little brown bat (*Myotis lucifugus*). *Biochem. Syst. Ecol.* **37**, 154-161. doi:10.1016/j.bse.2009.03.001

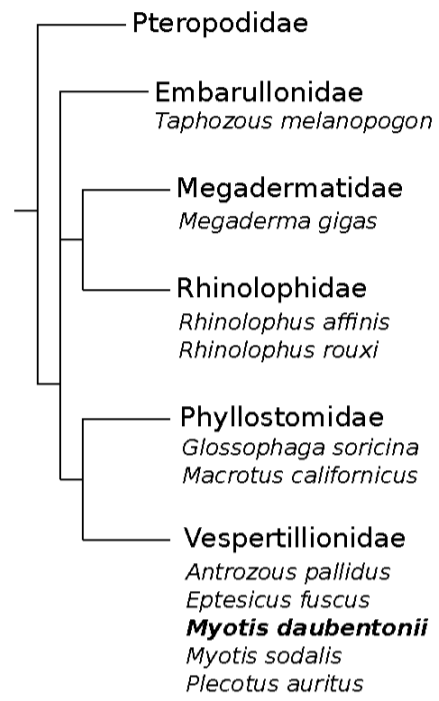


**Fig. S1.** Phylogenetic tree showing the relation between the different families of bats cited in this paper as well as the species within those families.

**Table S1.** Results from other studies on the acuity and sensitivity of the bat species cited in this study.

Family	Species	Ecology	Approximate eye size (mm)	Sensitivity measure		Acuity measure		Reference
				Method	Value	Method	Value (cycles/deg)	
Embarullonidae	<i>Tazophus melanopogon</i>	Insectivorous		Optomotor response	$6 \times 10^{-4}$ candela/m <sup>2</sup>	Optomotor response	0.25	Bell and Fenton, 1986
				Flash evoked potentials	$2 \times 10^{-4}$ candela/m <sup>2</sup>			Liu et al. 2015
Megadermatidae	<i>Megaderma gigas</i>	Insectivorous	7			Ganglion cell counts	2	Pettigrew et al., 1988
Phyllostomidae	<i>Glossophaga soricina</i>	Nectivorous		Behavioural threshold	$7.6 \times 10^9$ photons/cm <sup>2</sup> /s <sup>-1</sup>			Winter et al., 2003
	<i>Macrotus californicus</i>	Frugivorous		Optomotor response	$2 \times 10^{-4}$ mL	Optomotor response	17	Bell and Fenton, 1986
Rhinolophidae	<i>Rhinolophus affinis</i>	Insectivorous		Flash evoked potentials	$1.2 \times 10^{-2}$ candela/m <sup>2</sup>			Liu et al. 2015
	<i>Rhinolophus rouxi</i>	Insectivorous	1.8			Ganglion cell counts	0.2	Pettigrew et al., 1988
Vespertilionidae	<i>Antrozous pallidus</i>	Insectivorous		Optomotor response	$6 \times 10^{-4}$ candela/m <sup>2</sup>			Bell and Fenton, 1986
	<i>Eptesicus fuscus</i>	Insectivorous		Brightness discrimination	$10^{-4}$ candela/m <sup>2</sup>			Ellins and Masterson, 1974
	<i>Myotis daubentonii</i>	Insectivorous	1.2			Optomotor response	1	Bell and Fenton, 1986
	<i>Plecotus auritus</i>	Insectivorous	1.7			Ganglion cell counts	0.6	Céchetto et al., 2020
						Optomotor response	1.3	Eklöf et al., 2014



**Table S2.** Number of trials that were used to calculate the probability of success for each point in figure 2.

Light level (candela/m <sup>2</sup> )	Number of trials used to calculate probability			
	A	B	C	D
$2.16 \times 10^{-2}$	86	60	34	17
$1.08 \times 10^{-2}$	18	13	12	10
$5.43 \times 10^{-3}$	21	13	11	10
$2.72 \times 10^{-3}$	28	11	12	12
$1.08 \times 10^{-3}$	31	12	13	16
$5.43 \times 10^{-4}$	32	17	12	18
$2.72 \times 10^{-4}$	29	23	11	16
$2.16 \times 10^{-4}$	24	26	12	12
$1.72 \times 10^{-4}$	26	24	18	9
$6.83 \times 10^{-5}$	24	23	16	8
$3.42 \times 10^{-5}$	18	16	10	7
$2.16 \times 10^{-5}$	13	7	5	5
$1.72 \times 10^{-5}$	12	2	3	2
$1.08 \times 10^{-5}$	10	4	5	
$8.60 \times 10^{-6}$	4	3	1	
$5.43 \times 10^{-6}$	5	1		
$2.72 \times 10^{-6}$	4			
$6.83 \times 10^{-7}$				
$2.16 \times 10^{-7}$				

**Table S3.** Parameters values ( $\alpha$  and  $\beta$ ) used to fit the Weibull cumulative distribution function (Equation 2) to the data, and estimated threshold at 75% probability in in  $\log_{10}$  candela/m<sup>2</sup>. Bats A-D correspond to bats A-D shown in Figure 2A-D. Tables

Bat	$\alpha$	$\beta$	Threshold
A	-2.76	-3.33	-3.08
B	-3.53	-14.45	-3.62
C	-3.36	-6.70	-3.68
D	-3.14	-4.88	-3.40